World Academy of Science, Engineering and Technology
International Journal of Civil and Environmental Engineering
Vol:11, No:5, 2017

Numerical Model of Low Cost Rubber Isolators for Masonry Housing in High Seismic Regions

Ahmad B. Habieb, Gabriele Milani, Tavio Tavio, Federico Milani

Open Science Index, Civil and Environmental Engineering Vol:11, No:5, 2017 publications.waset.org/10007169/pdf

***Abstract*—**Housings in developing countries have often inadequate seismic protection, particularly for masonry. People choose this type of structure since the cost and application are relatively cheap. Seismic protection of masonry remains an interesting issue among researchers. In this study, we develop a low-cost seismic isolation system for masonry using fiber reinforced elastomeric isolators. The elastomer proposed consists of few layers of rubber pads and fiber lamina, making it lower in cost comparing to the conventional isolators. We present a finite element (FE) analysis to predict the behavior of the low cost rubber isolators undergoing moderate deformations. The FE model of the elastomer involves a hyperelastic material property for the rubber pad. We adopt a Yeoh hyperelasticity model and estimate its coefficients through the available experimental data. Having the shear behavior of the elastomers, we apply that isolation system onto small masonry housing. To attach the isolators on the building, we model the shear behavior of the isolation system by means of a damped nonlinear spring model. By this attempt, the FE analysis becomes computationally inexpensive. Several ground motion data are applied to observe its sensitivity. Roof acceleration and tensile damage of walls become the parameters to evaluate the performance of the isolators. In this study, a concrete damage plasticity model is used to model masonry in the nonlinear range. This tool is available in the standard package of Abaqus FE software. Finally, the results show that the low-cost isolators proposed are capable of reducing roof acceleration and damage level of masonry housing. Through this study, we are also capable of monitoring the shear deformation of isolators during seismic motion. It is useful to determine whether the isolator is applicable. According to the results, the deformations of isolators on the benchmark one story building are relatively small.

***Keywords*—**Masonry, low cost elastomeric isolator, finite element analysis, hyperelasticity, damped non-linear spring, concrete damage plasticity.

I. Introduction

SEISMIC isolation is a popular research topic since several seismic events in the recent past often lead to many casualties. As a matter of fact, seismic isolation can be a valuable solution to mitigate the negative impact that an earthquake can have on a building, because it shifts the period of the structure on that range of the spectrum where the spectral acceleration is low.

Masonry is a common type of housing in developing countries [1]. It typically consists of clay bricks bonded by sand and cement mortar. Without frames resisting moment, masonry construction relies on its shear strength of wall to resist the seismic load. Unfortunately, conventional bricks masonry has poor tensile strength, so its capacity to carry horizontal load is considerably reduced. In contrast with masonry poor performance against horizontal loads, it is still the preferred material in developing countries, because of the limited cost of construction. In many cases of earthquake events in Indonesia, low-class housings experienced severe damage, leading to several casualties [2]. This fact justifies the importance of conceiving a new seismic isolation system with low cost for low class housing.

A well known seismic isolation device is the elastomeric isolators. Typically, this isolator involves several layers of rubber and steel or fiber lamina as the reinforcement. This isolator has a capability to deform in the horizontal direction during seismic motion due to its low horizontal stiffness. This system can isolate the energy transmission of the earthquake from the foundation to the upper-structure. Meanwhile, the role of steel or fiber lamina between rubber layers is to improve the vertical stiffness of the isolator [3]. Some works employed fiber lamina to make the cost of the isolator cheaper [4], [5] and even used recycled rubber from tyres or industrial waste [6], [7].

The objective of this paper is to present the behavior of a new low-cost fiber reinforced elastomeric isolator (FREI). We consider models of FREI in smaller dimension comparing to the ones used in a previous experimental study [8]. After having deduced the shear behavior of the isolator by means of a detailed 3D FE approach, we model the isolator embedded in the entire structure as a damped non-linear spring. As seen in Fig. 1 (b), the identified spring represents the shear behavior of the isolator at a structural level. This method leads to a simpler computation in FE analyses rather than involving a detailed isolator on the masonry. Previous research recommends this way to model a structure isolated with elastomers [9]. In the end, we verify whether the model proposed is suitable for a one story masonry building prototype.

An elastomeric isolator exhibits different behaviors; in horizontal, vertical, and rotational direction. Apparently, the masonry building may not generate a rotational motion on the isolator since the structure uniformly distributes the horizontal and vertical loads. Meanwhile, in a moment resisting frame construction, the rotational behavior of the isolator may be considerable. We evaluate the applicability of isolators by observing the maximum axial and shear displacement. Once the isolator starts to deform horizontally, its axial capacity decreases. It is due to the reduction of rubber pad surfaces that undergo the axial load.

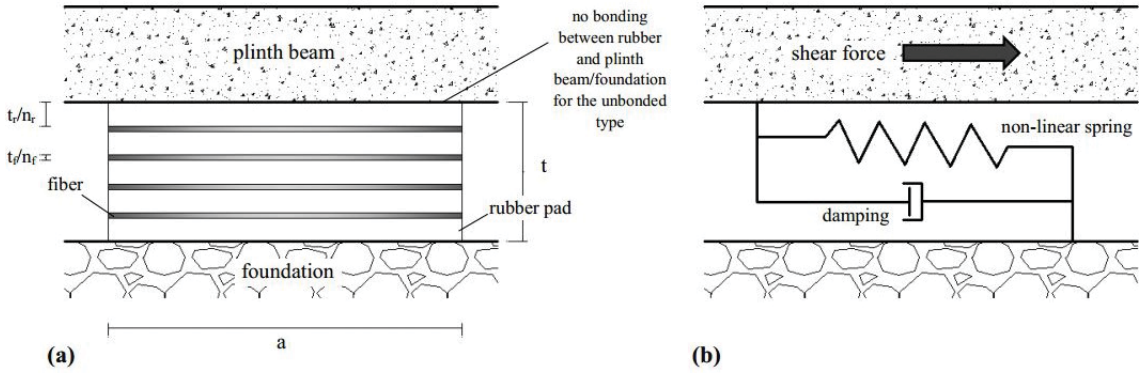
To model the behavior of rubber, we use a hyperelastic material model that is available in standard Abaqus FE software. Thanks to its simplicity, we utilize a Yeoh

A. B. Habieb and G. Milani are with the Department of Architecture, Building, and Construction Engineering, Politecnico di Milano, 20158 Milano, Italy (corresponding author, e-mail: ahmadbasshofi.habieb@polimi.it).

Tavio Tavio is with Civil Engineering Department, Institut Teknologi Sepuluh Nopember, 60111 Surabaya, Indonesia.

F. Milani is with Chem. Co Consultant, Via J. F. Kennedy 2, 45030 Occhiobello (RO), Italy.

Open Science Index, Civil and Environmental Engineering Vol:11, No:5, 2017 publications.waset.org/10007169/pdf



a/b = isolator length/width
t = isolator total thickness
t_r = total rubber pads thickness
n_r = number of rubber pads
t_f = total fiber laminas thickness
nf = number of fiber laminas
S = shape factor

Dimensions (mm) of the isolators considered

Isolator	a	b	t	t_r/n_r	t_f/n_f	S
FREI 100	100	100	56	10	1.5	2.5
FREI 150	150	150	56	10	1.5	3.75
FREI 200	200	200	105	4.7	0.5	10.6

Fig. 1 (a) Geometry of the elastomeric isolator and (b) the representative damped spring model

hyperelastic model to characterize rubber properties [10]. Meanwhile, the fiber lamina behaves as an elastic material [5]. For masonry, we employ the concrete damage plasticity (CDP) which is available in standard Abaqus. Failure behavior of masonry is more related to the mortar since its tensile strength is lower than that of the brick. During seismic motion, we observe roof acceleration and damage propagation into the masonry model. From simulation results, it turns out that the isolation system may reduce the roof acceleration and damage level of the brick wall. In the end, we compare the performance between the isolators proposed in terms of damage propagation on masonry and maximum roof accelerations.

II. Finite Element Model

A. Numerical Model of Fiber Reinforced Elastomeric Isolator

Hyperelasticity is an important issue in this study to define the behavior of the elastomeric isolator. Some researchers proposed models of hyperelasticity based on the strain energy function. In this study, properties of the rubber follow the Yeoh hyperelastic model due to its simplicity of computation. Equation 1 expresses the Yeoh model for a compressible rubber material [11] and Table I shows the coefficients in our FE model.

TABLE I
Coefficients of Yeoh Model in Abaqus

C_{10}	C_{20}	C_{30}	D_1	D_2	D_3
0.2551	0.0066	0.000032	0.00218	8.68E-05	-1.794E-05

C in MPa

$$W = \sum_{i=1}^{3} C_{i0}(I_1 - 3)^i + \sum_{i=1}^{3} \frac{I}{D_i}(J_{el} - 1)^{2i} \qquad (1)$$

where W is the strain energy per unit of volume; C_{i0} and D_i are material parameters; I_1 is the first deviatoric strain invariant; and J_{el} is the elastic volume ratio.

We estimate these coefficients by referring to a previous paper [12]. That paper evaluates the Yeoh coefficients of rubber materials with different hardness. In this work, we use the same rubber material examined in the earlier study [8], with a Shore A hardness equal to 40. Elastomeric isolators discussed in this work use fibers as the reinforcement to improve the vertical stiffness. It has been shown indeed, that fibers can reduce the cost of the isolator when compared with steel lamina [13], [7]. In this numerical simulation, we consider the fiber as an elastic material with Young modulus E = 40000 MPa and Poisson's ratio = 0.25.

Fig. 1 (a) introduces the dimension of three isolators we propose. The FREI-200 is an isolator tested at McMaster University (Hamilton, Canada) [8]. We consider it as a reference sample. Its side is 200 mm both in length and width. Two other specimens are isolators we propose, with much smaller dimension than the previous one. FREI-150 and FREI-100 have only five pads of rubber with 10 mm of

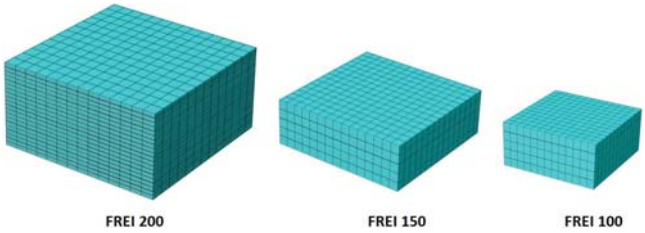


Fig. 2 Size comparison of isolators considered and meshing of FE model

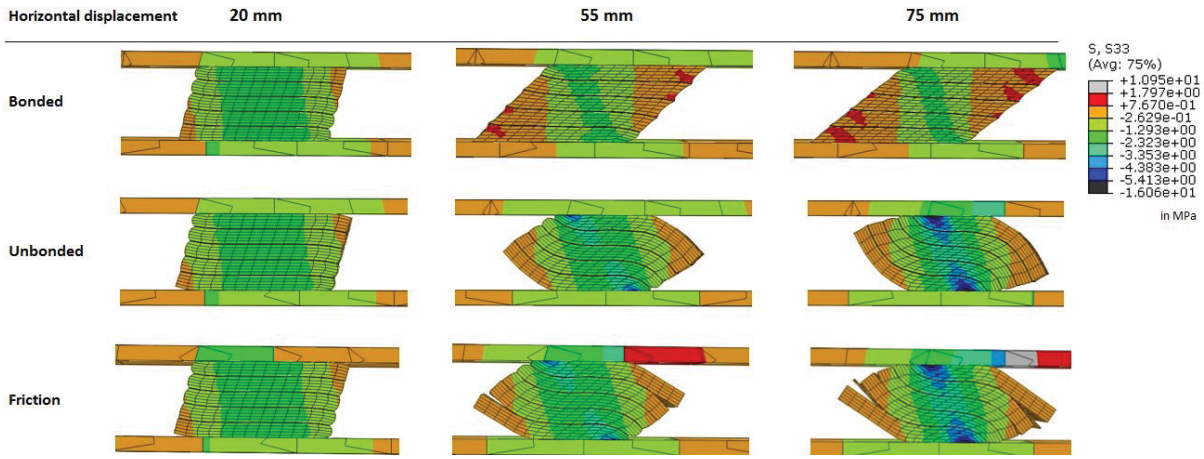


Fig. 3 Deformation and stress of bonded, unbonded, and frictional isolator FREI 100

thickness, while the FREI-200 has 20 pads with 4.7 mm of thickness. Fig. 2 shows the size comparison of isolators and mesh of the FE models using C3D8R element.

We perform horizontal displacement analyses under geometric and material non-linear hypotheses, applying a constant vertical load on the upper surface of the isolator, to observe its shear behavior. First, we simulate three conditions; bonded, unbonded and frictional isolator (Fig. 3). In bonded model, the surface of elastomer and the upper and bottom supports are tied. It is the first common type of base isolator which requires thick steel plates for the supports. Thus, we can not consider it as a low-cost device. Once a large displacement takes places, excessive tensile stresses appear (Fig. 3), leading to the damage of rubber-reinforcement interface (which is not reproducible with such FE model). The second is the unbonded elastomer, where the surfaces do not have bonding to the supports. In moderate shear force, this frictional limited strength allows the isolator to roll over and facilitates a larger deformation. Unlike the previous model, rubber tensile stresses strongly decrease. The last numerical prototype we propose is the frictional isolator. It does not require any bonding, even between rubbers and fibers. A paper discusses this type in application of recycled tyre rubber [14]. Like the unbonded elastomer, it can undergo roll-over deformation in moderate displacement. But it seems not able to resist high horizontal deformation since the layers will be detached, as seen in Fig. 3. For the sake of conciseness, in this paper we discuss only the performance of the unbonded elastomer in isolating a masonry structure.

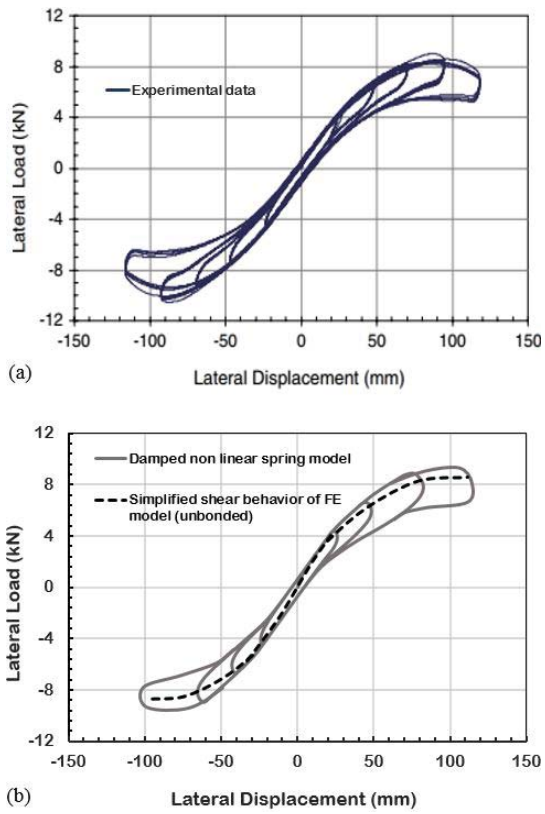


Fig. 4 (a) Experimental shear behavior of FREI-200, (b) Shear behavior of FREI-200 by FE model and representative damped-spring model

In this simulation, we consider that a single isolator is subjected to a vertical load of 0.83 tons. This is because the masonry building prototype is 10 tons and we dispose 12 isolators on the foundation, see Fig. 7 (a). To realistically reproduce experimental results, it is needed to generate the hysteresis behavior of the isolators. Two of the authors of this paper proposed a hysteresis behavior of the FE model by implementing elastoplastic and hyperelastic properties [15]. In the present paper, we adopt a similar procedure. First, we generate a nonlinear behavior of the FE model without different loading-unloading paths, see Fig. 4 (b) . The dashed line is the shear behavior obtained by the FE analysis of unbonded FREI-200. Having this displacement-load curve, we input it as the properties of a nonlinear spring. To generate the hysteresis behavior, we apply a damping coefficient to the spring. In this case, a value of 10% damping fits the model from experimental data (Fig. 4 (a)). Thus, we adopt this damping coefficient also for two other FE models. For FREI-150 and FREI-100, Figs. 5 (a) and (b) show the shear behavior and the corresponding model adopted for the identified non-linear spring.

Open Science Index, Civil and Environmental Engineering Vol:11, No:5, 2017 publications.waset.org/10007169/pdf

Open Science Index, Civil and Environmental Engineering Vol:11, No:5, 2017 publications.waset.org/10007169/pdf

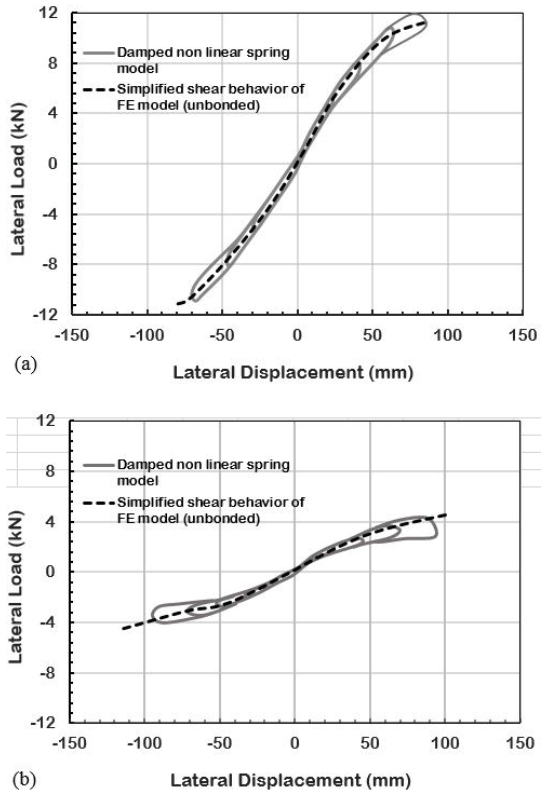


Fig. 5 Shear behavior of FE unbonded model and representative damped-spring model for (a) FREI-150 and (b) FREI-100

Such identification procedure satisfies the simplified model introduced in Fig. 1. Modeling a spring instead of a real 3D isolator makes the computation more efficient. Furthermore, we are capable of simulating a masonry structure with a realistic representation of the isolation system.

B. FE Model of an Isolatod Masonry House Prototype

We consider a model of a one-story masonry building with openings. The dimensions of the building are 150 mm in wall thickness, 4 m x 4 m in length and 3m in height, see Fig. 7 (a). Also, the weight of the roof is 30 kg/m^2. To prevent the flexural damage of the walls, some rigid beams on top of the windows and the door are present.

In modelling masonry, we consider it as an isotropic material. Even this is a simplification, it is commonly accepted in engineering practice [16], [17], also because commercial FE codes have rarely at disposal orthotropic damaging materials in their standard packages. To determine the non-linear behavior, we adopt a concrete damage plasticity model (CDP). This model is available in the standard package of Abaqus FE

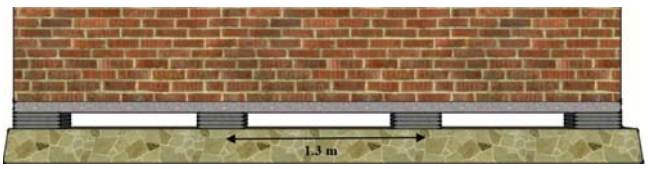


Fig. 6 Masonry structure isolated with unbonded elastomeric isolators

TABLE II
VALUES OF THE MECHANICAL PARAMETERS ADOPTED FOR FE MODEL

Dilatation angle	Eccentricity	σ_{b0}/σ_{c0}	K_c	Viscocity
10	0.1	1.16	0.667	0.0001

software and compatible with the nonlinear behavior of brittle or quasi-brittle materials such as concrete and therefore masonry.

The CDP model requires data on non-linear behavior in uniaxial tension and compression. For this study, the simplified axial stress-strain relationships shown in Figs. 7 (b) and (c) are utilized. The tensile damage determines mainly the overall state of damage of the masonry prototype, since mortar tensile strength is considerably low. The stress-strain relation in tension exhibits a peak strength of σ_{t0} = 0.15 MPa for the unreinforced masonry. This value corresponds to the tensile strength of mortar. Then micro-cracks start to propagate within the material, leading to a macroscopic softening. In compression (Fig. 7(c)), the response is linear up to the yield stress σ_{c0}= 1.8 MPa, followed by a cruising stress σ_{cu}=2.4 MPa and linear softening branch. Then we input other parameters of CDP obtained from a previous research [16] as seen in Table II.

Masonry structures are vulnerable to the horizontal action due to the absence of moment resisting frames. Retrofitting or isolating the masonry construction are required to assure the safety of the building. Technological details of masonry isolation remains an interesting issue to discuss. We consider a one story masonry housing as the sample of this simulation. To facilitate the application of base isolator, we placed rigid beams along the base of the walls. This configuration let the elastomeric isolator stand between the foundation and the upper structure (Fig. 6).

In this FE analysis, the number of isolators involved is 12 with equally stepped distance, see Fig. 7 (a). We already have the damped nonlinear spring model of the isolator to implement in the simulation. The building is subjected to some some earthquake loads with different peak ground accelerations (PGA). In this simulation, we also examine the performance of each isolator in terms of isolation capability and reduction of damage on the superstructure. In low-rise masonry structures, it is worth noting that we may neglect neglect the rotational behavior of isolators, since the distributions of vertical and horizontal load are uniform.

III. PERFORMANCE OF THE ISOLATORS ON MASONRY HOUSING

After the application of the seismic load within a non-linear dynamic analysis, it is possible to appreciate the structural behavior of masonry with or without isolation. Fig. 8 shows the acceleration responses of the building due to L'Aquila earthquake (PGA=0.6). Without seismic protection, the reference point on the roof level accelerates much more that the base, where the accelerogram is applied. It indicates that the masonry wall deflects considerably, with probable generation of diffused tensile damage of the superstructure.

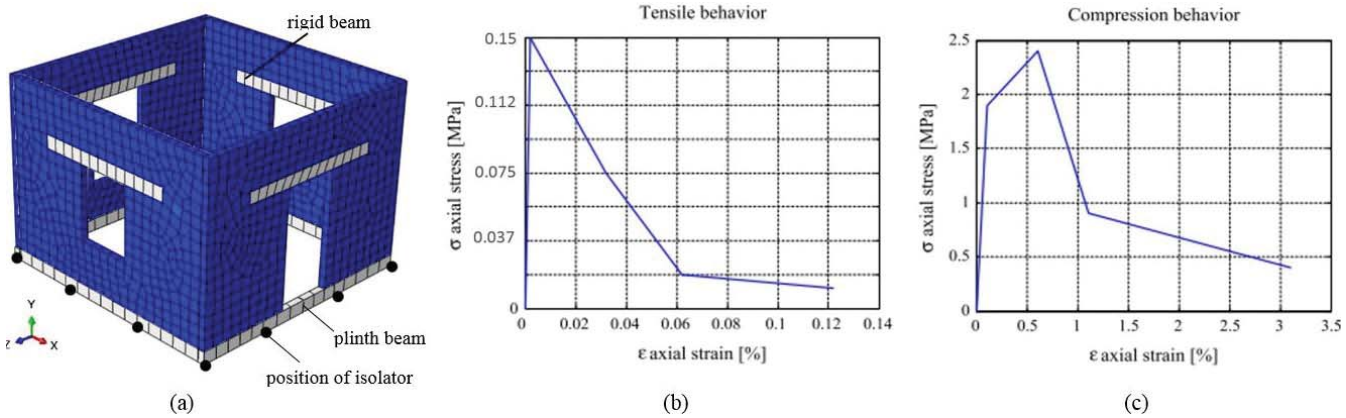


Fig. 7 (a) Mesh of masonry housing and isolators configuration, (b) simplified nonlinear behavior in uniaxial tension and (c) in compression

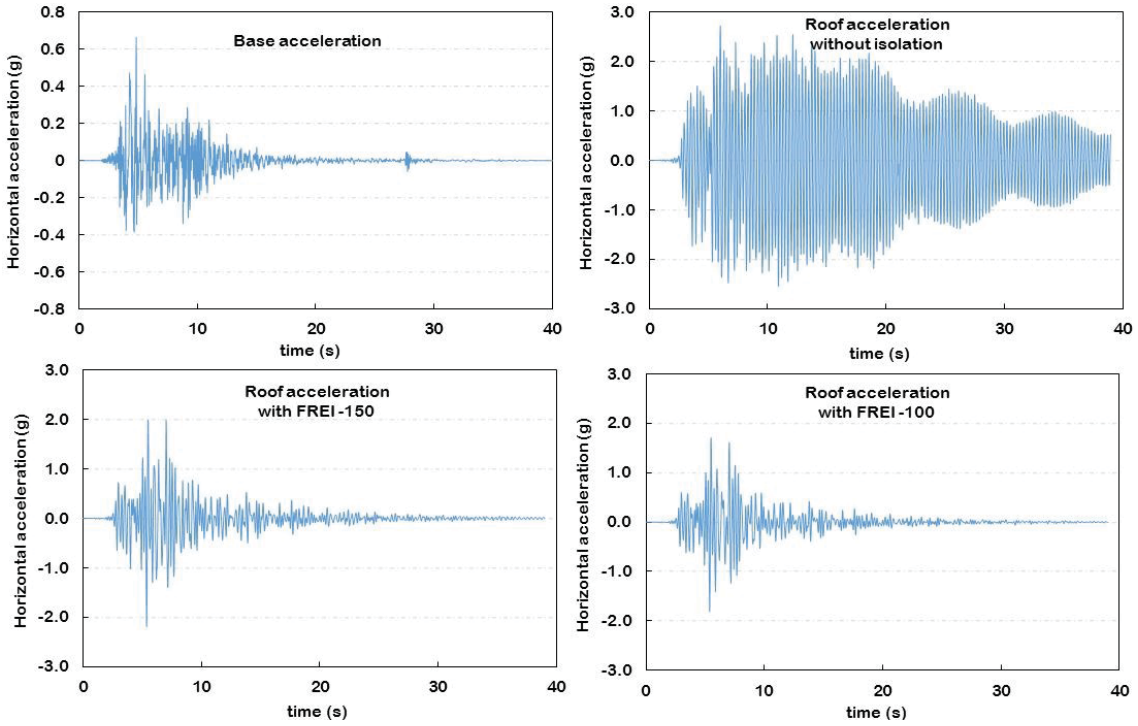


Fig. 8 Acceleration responses of masonry housing without and with elastomeric isolators due to L'aquila earthquake

On the contrary, the utilization of the isolators results in a mitigation of the roof accelerations, with reduction of damage.

The software used in this study is capable of illustrating the damage level of the building as seen in Fig. 9. When the level of damage reachs 0.925, the material undergoes 0.003 of tensile strain, which corresponds to mortar total cracking. Fig. 9 visually gives an idea of the different levels of damage reached on the superstructure applying Tabas accelerogram. In Tabas earthquake, the unisolated one suffers tensile damage approximately up to 80% of its entire volume. Whereas, only about 10% damage appears in all isolated models. In masonry structures under seismic excitation, damage in compression does not play an important role in determining the failure behavior. Thus we do not discuss it in this work.

Examining some earthquake data, Fig. 10 (a) shows with histograms the global damage obtained applying different real accelerograms for the isolated and non-isolated systems. L'Aquila earthquake with 0.6g of PGA seems to result in less damage even lower than El-Centro earthquake with 0.25g. Ground motion in L'Aquila earthquake may have a large acceleration but with a short duration as seen in Fig. 8. In this one-story masonry case, the different dimension of the three isolators apparently does not influence the level of protection. All isolator models have the same capability in reducing damage so that the smallest one may be the most efficient device to use in this case.

Also, we are able of monitoring horizontal deformation of the isolators. Fig. 10 (b) gives the graph of maximum shear deformation of the isolator. This maximum deformation evaluates whether the device is applicable. The largest deformation takes place in FREI-100 during Tabas earthquake, which is 30 mm. However, we will discuss the deformation

Open Science Index, Civil and Environmental Engineering Vol:11, No:5, 2017 publications.waset.org/10007169/pdf

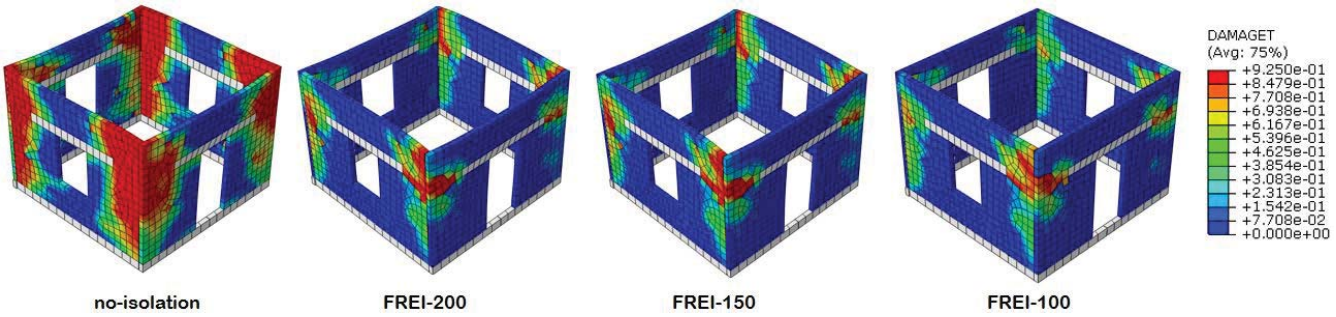


Fig. 9 Level of tensile damage in masonry housing with different isolators due to Tabas Earthquake (PGA = 0.86g)

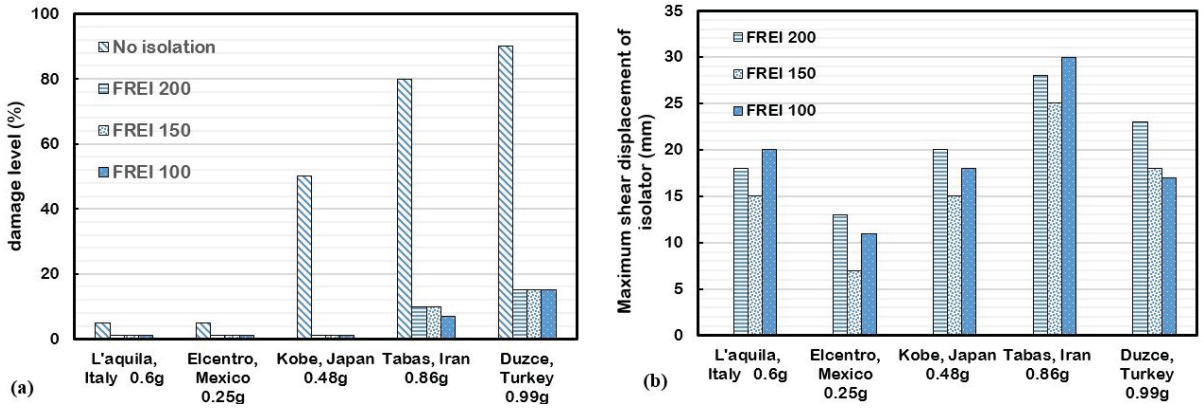


Fig. 10 Comparative graphs of (a) damage level, and (b) maximum shear displacement of isolators due to several seismic cases

limit of the low-cost elastomeric isolator in another work.

IV. Conclusions

We carried out 3D FE analyses on low-cost fiber reinforced elastomeric isolators of several types; bonded, unbonded, and frictional elastomer. The isolators proposed have considerably smaller dimensions comparing to the conventional isolator. The unbonded one seems not applicable on low-cost seismic isolation due to excessive tensile stress and need of adhesive. Having in mind of applying this isolation system in medium to high seismicity regions, we recommend the unbonded one for the isolation of low rise masonry buildings. Such type of isolator indeed, may facilitate a moderate horizontal deformation during an earthquake, fairly reducing damage on masonry superstructure. .

To simplify the numerical analysis, modeled the isolator at a structural level as a damped nonlinear spring to apply at the base of the superstructure. This simplified method works and leads to a faster computation rather than modeling the real 3D geometry of the isolators into FEs. However, this work needs an experimental validation to verify the accuracy of the method proposed. Another potential issue is to develop and investigate a low-cost isolation system for mid-rise masonry buildings, considering the horizontal and rotational stability of the isolator.

Acknowledgment

The authors would like to acknowledge the financial support from LPDP Scholarship, Finance Ministry of Indonesian Republic for sponsoring Mr. Ahmad B. Habieb to study at Politecnico di Milano, Italy.

References

[1] R. P. Nanda, M. Shrikhande, and P. Agarwal, "Low-cost base-isolation system for seismic protection of rural buildings," *Practice Periodical on Structural Design and Construction*, vol. 21, no. 1, p. 04015001, 2015.
[2] T. Boen, *Yogya Earthquake 27 May 2006: Structural Damage Report*. EERI, 2006.
[3] J. M. Kelly, "Earthquake-resistant design with rubber," 1993.
[4] A. Das, S. K. Deb, and A. Dutta, "Shake table testing of un-reinforced brick masonry building test model isolated by u-frei," *Earthquake Engineering & Structural Dynamics*, vol. 45, no. 2, pp. 253–272, 2016.
[5] N. C. Van Engelen, P. M. Osgooei, M. J. Tait, and D. Konstantinidis, "Experimental and finite element study on the compression properties of modified rectangular fiber-reinforced elastomeric isolators (mr-freis)," *Engineering Structures*, vol. 74, pp. 52–64, 2014.
[6] A. Turer and B. Özden, "Seismic base isolation using low-cost scrap tire pads (stp)," *Materials and Structures*, vol. 41, no. 5, pp. 891–908, 2008.
[7] M. Spizzuoco, A. Calabrese, and G. Serino, "Innovative low-cost recycled rubber–fiber reinforced isolator: experimental tests and finite element analyses," *Engineering Structures*, vol. 76, pp. 99–111, 2014.
[8] H. Toopchi-Nezhad, M. J. Tait, and R. G. Drysdale, "Testing and modeling of square carbon fiber-reinforced elastomeric seismic isolators," *Structural Control and Health Monitoring*, vol. 15, no. 6, pp. 876–900, 2008.
[9] M. Kumar, A. S. Whittaker, and M. C. Constantinou, "An advanced numerical model of elastomeric seismic isolation bearings," *Earthquake Engineering & Structural Dynamics*, vol. 43, no. 13, pp. 1955–1974, 2014.
[10] M. Shahzad, A. Kamran, M. Z. Siddiqui, and M. Farhan, "Mechanical characterization and fe modelling of a hyperelastic material," *Materials Research*, vol. 18, no. 5, pp. 918–924, 2015.
[11] D. Simulia, "Abaqus 6.13 users manual," *Dassault Systems, Providence, RI*, 2013.

Open Science Index, Civil and Environmental Engineering Vol:11, No:5, 2017 publications.waset.org/10007169/pdf

[12] S. Jerrams, M. Kaya, and K. Soon, "The effects of strain rate and hardness on the material constants of nitrile rubbers," *Materials & design*, vol. 19, no. 4, pp. 157–167, 1998.
[13] A. Calabrese, M. Spizzuoco, G. Serino, G. Della Corte, and G. Maddaloni, "Shaking table investigation of a novel, low-cost, base isolation technology using recycled rubber," *Structural Control and Health Monitoring*, vol. 22, no. 1, pp. 107–122, 2015.
[14] H. K. Mishra, A. Igarashi, and H. Matsushima, "Finite element analysis and experimental verification of the scrap tire rubber pad isolator," *Bulletin of Earthquake Engineering*, pp. 1–21, 2013.
[15] G. Milani and F. Milani, "Stretch–stress behavior of elastomeric seismic isolators with different rubber materials: numerical insight," *Journal of Engineering Mechanics*, vol. 138, no. 5, pp. 416–429, 2011.
[16] T. Choudhury, G. Milani, and H. B. Kaushik, "Comprehensive numerical approaches for the design and safety assessment of masonry buildings retrofitted with steel bands in developing countries: The case of india," *Construction and Building Materials*, vol. 85, pp. 227–246, 2015.
[17] S. Tiberti, M. Acito, and G. Milani, "Comprehensive fe numerical insight into finale emilia castle behavior under 2012 emilia romagna seismic sequence: damage causes and seismic vulnerability mitigation hypothesis," *Engineering Structures*, vol. 117, pp. 397–421, 2016.

Open Science Index, Civil and Environmental Engineering Vol:11, No:5, 2017 publications.waset.org/10007169/pdf